# Multifragmentation of the $Au(H_2O)_{n\leq 10}^+$ Cluster Ions by Collision with Helium

**L. Poisson,† F. Lepetit, J.-M. Mestdagh,* and J.-P. Visticot**

*Laboratoire Francis Perrin (CNRS URA 2453) CEA/DRECAM/Service des Photons, Atomes et Molécules, C. E. Saclay, F-91191 Gif-sur-Yvette Cedex, France*

*Received: January 25, 2002*

A beam of mass selected $Au(H_2O)_n^+$ ($n = 1-10$) cluster ions has been generated using a source that couples laser evaporation, supersonic expansion, and tandem time-of-flight mass spectrometry. A collision-induced-dissociation (CID) experiment has been performed with helium at energies in the range of 0.2−3 eV. A maximum of four water molecules is lost by the clusters. The key point is the data analysis where the total (loss of at least one water molecule) and partial (loss of a specified number of water molecules) CID cross sections have been simulated using a model describing the energy transfer between helium and the cluster. This has allowed us to fit the experimental data and to give insight into the structure and energetic of the $Au(H_2O)_n^+$ clusters, unraveling the existence of two kinds of isomers for these clusters, one with two water molecules coordinating the metal ion, tentatively assigned to $(H_2O)_p(H_2O)Au^+(H_2O)(H_2O)_{n-p-2}$, and a more compact one with three (or more) coordinating water molecules. Multifragmentation of $Au(H_2O)_{n\geq 6}^+$ clusters seems to involve a competition between the sequential loss of several water molecules and the loss of a water dimer and possibly a trimer.

## 1. Introduction

Hydrated metal ions are involved in many chemical and biological phenomena, hence motivating a lot of attention. In particular, cluster ions of the form $M(H_2O)_n^+$ can be considered as valuable models for studying the solvation of a metal ion $M^+$ by water at a microscopic level.[1] Of course, the connection with bulk water phenomena is best studied when considering clusters beyond the first solvation shell about the metal ion. Such clusters are also interesting in their own, and their experimental study is made possible by the availability of various techniques to generate routinely such large clusters: supersonic expansion coupled to a pick-up,[2−8] coupling between laser evaporation and supersonic expansion.[9−11]

An important question regarding the $M(H_2O)_n^+$ clusters, whatever the value of *n*, is their structure and energetics. Fragmentation is often used to probe such properties, especially collision-induced-dissociation (CID).[12] For instance, the binding energy of water in $M(H_2O)_n^+$ clusters has been extensively documented by CID, performing threshold energy measurements in a guided ion beam tandem mass spectrometer, and using a heavy atom, xenon, as target gas.[13] The reason for choosing xenon is to transfer the collision energy into the entire cluster, which then dissociates through a RRKM-like process. A careful examination of the effects that bias the threshold energy measurements[13] plus the modelization of the dissociation rate[14,15] allows one to correct threshold energy measurements, hence providing an accurate determination of the binding energies.

Recently, helium, which is a light and small size target, has been used in our laboratory to induce dissociation of $Fe(H_2O)_2^+$, $Co(H_2O)_2^+$, and $Au(H_2O)_2^+$ cluster ions.[16] In that case, energy is deposited very inhomogeneously within the cluster, essentially because helium transfers most of its energy into H atoms and not into the heavier constituents of the cluster. This has been modelized by a molecular dynamics calculation, which takes into account the inhomogeneous structure of the $M(H_2O)_n^+$ clusters.[17] It appears that the energy transfer is more efficient toward an H atom which is not involved in an H bond (up to 90% efficiency) than toward H-bonded H atoms (a maximum efficiency of 60%). [Note that the term "H bond" which is used here and throughout the text is simply a convenient fashion to indicate that two water molecules are bonded together. It does not refer to the exact geometry and binding energy of the water dimer. In particular, we shall see along this paper that the binding energies between such "H-bonded" water molecules differ significantly from that of a "true H bond" in the water dimer.] These calculations have provided the framework to predict the shape of CID cross sections above the threshold energy for dissociation. Hence, the full data analysis in CID experiments using helium as target gas does not reduce to the analysis of the threshold region, which is often ill-defined experimentally. Instead, it focuses the attention on the energy dependence of the cross section above threshold. This was exemplified in a study of the $Co(H_2O)_n^+$ and $Fe(H_2O)_n^+$, for $n = 1-10$.[18] [Incidentally, but this is not essential here, the CID experiments of ref 18 were complemented by photofragmentation experiments. It was shown that CID documents the overall shape of the cluster, whereas photofragmentation informs on the response of the metal ion to its local environment.]

The present work aims at examining the loss of one or several water molecules from $Au(H_2O)_n^+$ clusters in collision with helium, with n ranging between 1 and 10. Small $Au(H_2O)_n^+$ clusters with $n = 1$ and 2 have been studied already, both experimentally[16,19−21] and theoretically,[22] but to our knowledge, larger clusters have not been investigated yet experimentally. In contrast, clusters with $n \leq 4$ have be explored theoretically.[22] By examining both total CID cross sections, i.e., disregarding the number of water molecules that are lost, and partial cross sections corresponding to the loss of a specified number of water

* Corresponding author: FAX 33-1-69-08-84-46, email jmm@drecam.saclay.cea.fr.

† Present address: Lawrence Berkeley National Laboratories, 6-2100 ALS, Chemical Science Division, Berkeley, CA 94720.

10.1021/jp025557a CCC: $22.00 
Published on Web 05/11/2002

molecules and using the calculations of Feller et al.[22] as guide line, it is hoped to get some experimental insight into the structure and energetics of the $Au(H_2O)_n^+$ cluster ions and also into the loss mechanism of one and several water molecules. The latter aim is in connection with a quite fundamental problem that has not received much attention yet for the inhomogeneous cluster: the dissipation of an excess internal energy by a microcanonical system that has been excited collisionally.[23]

## 2. Experiment

**Apparatus.** The apparatus has been described extensively in our former publications.[11,16,18,24] Briefly, a vaporization laser is focused on a metal rod (gold in the present case), generating $Au^+$ ions. The ions are carried by a helium/water jet into a supersonic expansion zone where the $Au(H_2O)_n^+$ cluster ions are generated. After the expansion, perpendicularly to the beam, the ions are extracted and accelerated using a pulsed Wiley−McLaren device operating with a 500 eV acceleration voltage. An electrostatic gate follows. It allows us to select cluster ions carrying a definite number of water molecules. $Au(H_2O)_n^+$ where $n = 1-10$ are considered in the present work.

After the gate, an assembly formed by a deccelerator, a collision cell, and an accelerator allows for running the CID experiments at a controlled collision energy. The collision cell is filled with helium at a controlled pressure. After this assembly, parent and fragment ions enter into a reflectron mass spectrometer and are analyzed and detected. An RF-octopole field is guiding the cluster ions in the collision cell in order to prevent ion losses. This, together with an accurate determination of both the interaction length and the helium pressure, allows us to determine absolute CID cross sections. As shown in ref 24, the CID experiments are run with the Wiley−McLaren device operating under the double extraction mode. This ensures enough mass resolution to the system to distinguish between parent and fragment ions after the collision.

**Time Window.** Time window is always an important question when measuring dissociation cross sections because an unsufficient time given to the ions to dissociate results into inaccuracies.

The time spent by the ions in the collision cell gives an order of magnitude of the time window for observing fragmentation in the present apparatus. This duration depends both on the cluster ion mass and on the collision energy that has been chosen for running the CID experiment. A typical value is 200 $\mu$s, which corresponds to a limiting dissociation rate of $5 \times 10^3$ $s^{-1}$, a quite small value. Above this limit, the dissociation can be considered as total. Below, cluster ions that nevertheless contain enough internal energy to dissociate do not have enough time to do so, before entering the reflectron mass spectrometer and being detected as an unfragmented species.

Because the present measurements focus the attention on the CID cross sections, well above the dissociation threshold where the dissociation rate is quite large, time window effects are not expected to cause significant troubles.

**Cross Section Measurements.** As in our former papers,[16,18] parent and fragment ion signals are recorded as a function of the helium pressure in the collision cell. A typical measurement is shown in Figure 1 for $Au(H_2O)_8^+$ at 1.79 eV collision energy in the center-of-mass reference frame.

A single-exponential behavior is expected for the parent and fragments when the single collision regime is achieved. Under this assumption, the parent ions decay as

$$\exp\left(-\sigma_{\text{tot}}\frac{P}{kT}L\right) \tag{1}$$

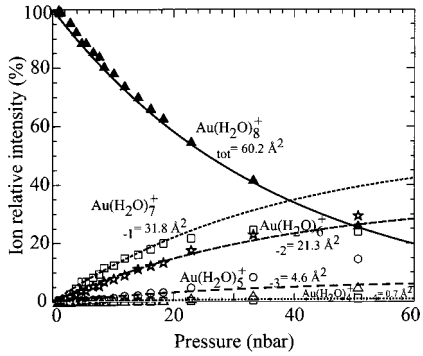


**Figure 1.** Relative intensity of the parent and fragment ion signals in a CID experiment where $Au(H_2O)_8^+$ is collided with helium at 1.79 eV collision energy in the center-of-mass reference frame. The ion signal are shown as a function of the helium pressure in the collision cell. The full lines displays the best fit to the experimental data, using expressions 1 and 2.

and the fragments are produced according to

$$\frac{\sigma_f}{\sigma_{\text{tot}}}\left[1 - \exp\left(-\sigma_{\text{tot}}\frac{P}{kT}L\right)\right] \tag{2}$$

In these expressions, $P$ and $T$ are respectively the pressure and the temperature of helium in the collision cell, $L$ is the length of the collision cell, and $k$ is the Boltzmann constant. $\sigma_{\text{tot}}$ and $\sigma_f$ are respectively the total CID cross section (disregarding which fragment is formed) and the partial cross section for forming the fragment $f$ ($f = -1, -2, -3$, etc. whether 1, 2, 3, etc. water molecules are lost).

Expressions 1 and 2 are used to fit signals such as those shown in Figure 1, at least at low enough helium pressure when the single collision regime is achieved. The cross sections $\sigma_{\text{tot}}$ and $\sigma_f$ are used as parameters in the fit because the other quantities in expressions 1 and 2 are controlled experimentally ($P$) or have a known value ($T$, $L$, and $k$). An example of such a fit is shown in Figure 1. It is of good quality over the full pressure range for the parent ion, whereas it is good only below 20 nbar for the fragments. The latter observation indicates that the multicollision regime begins to be efficient above this pressure, with the largest fragment, $Au(H_2O)_7^+$ being dissociated into smaller one by secondary collisions. The fact that the parent ion decay is still monoexponential at a pressure above 20 nbar shows that the dissociation has proceeded before a secondary collision has occurred, an indication that the dissociation rate exceeds the time window of the experiment in this case. From this, we know that the total CID cross section is unbiased by time window effects. This has been checked for the other cluster sizes and for the other collision energies explored in the present work.

Our former work on $Fe(H_2O)_n^+$ and $Co(H_2O)_n^+$ cluster ions has shown that the ion source can generate several isomers of the same cluster size.[18] Except at threshold, the total CID cross sections do not differ by orders of magnitude from one isomer to the other. This was the case for the $Fe(H_2O)_n^+$ and $Co(H_2O)_n^+$ cluster ions.[18] This is expected to be the case too with the $Au(H_2O)_n^+$ clusters. Hence, even if several isomers of the $Au(H_2O)_n^+$ cluster are present in the beam, the parent ion decay still appears as monoexponential, as exemplified in Figure 1. The value of $\sigma_{\text{tot}}$ and $\sigma_f$ that are fitted on the experimental data thus corresponds to an average over the isomer distribution present in the beam.

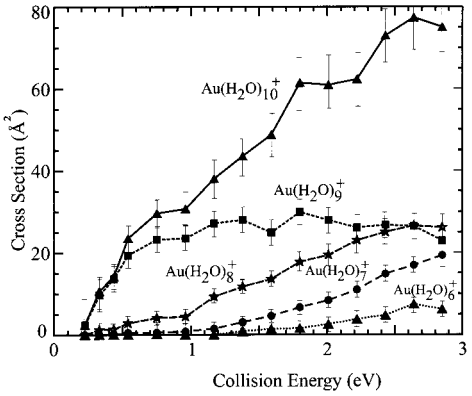


**Figure 2.** Total and partial CID cross sections of the $Au(H_2O)_{10}^+$ cluster ion as a function of the center of mass collision energy. The line going through the experimental points is for guiding the eyes.

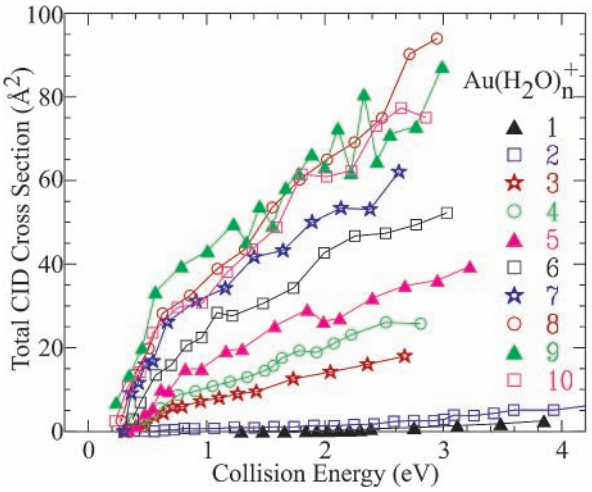


**Figure 3.** Total CID cross section of the $Au(H_2O)_n^+$ clusters as a function of the center of mass collision energy. The value of $n$ is indicated in the figure. Error bars have not been plotted for clarity. The line going through the experimental point is for guiding the eyes.

## 3. Results

Total and partial CID cross sections have been measured for the $Au(H_2O)_n^+$ ions ($n = 1-10$), as a function of the collision energy over the range of 0.2−3 eV in the center of mass reference frame.

Figure 2 displays the full results for the $Au(H_2O)_{10}^+$ cluster ion. Within error bars, the total CID cross sections increase steadily over the energy range of 0.2−3.0 eV. Four fragments are observed, corresponding to the loss of up to four water molecules. The loss of more than four water molecules does not lead to any measurable signal over the energy range that has been explored. The partial cross section for forming the $Au(H_2O)_9^+$ fragment is significant above 0.2 eV collision energy. It levels at ca. 25 Å$^2$ above 1 eV collision energy. Significant loss of two, three, and four water molecules starts at 0.5, 1.2, and 2 eV, respectively. The partial cross sections for the formation of these fragments do not level as that of $Au(H_2O)_9^+$. Instead, at 2.8 eV collision energy, the loss of two and three water molecules has reached about the same efficiency than the loss of one water molecule.

Figure 3 reports the total CID cross sections for the different sizes ($n = 1-10$) of the $Au(H_2O)_n^+$ clusters, as a function of the collision energy. The cross sections shown in Figure 3 fall into three categories:

(1) The CID cross section for $Au(H_2O)^+$ and $Au(H_2O)_2^+$ are extremely small but still accurately measurable. These curves have already appeared in ref 16 and 17 where they were compared to the prediction of the energy transfer model based on molecular dynamics calculation. The agreement was good. It allowed us to determine the binding energy of a second shell water molecule in the "low coordination" isomer $Au^+(H_2O)$-$(H_2O)$ of $Au(H_2O)_2^+$, which was not documented yet (0.4 ± 0.1 eV, see Table 1 which summarizes the water binding energies in the $Au(H_2O)_n^+$ ions). In this metastable isomer, the coordination number of $Au^+$ is one.

**TABLE 1: Binding Energy of the Most Weakly Bonded Water Molecules in the "Low" and "High" Coordination Isomers of the $Au(H_2O)_n^+$ Cluster Ions[a]**

| | incremental binding energy (eV) of the isomer with coordination number | | | |
|---|---|---|---|---|
| cluster ion | 1 | 2 | ≥3 | % |
| $Au(H_2O)^+$ | 1.74 ± 0.1<br>1.74[b]<br>1.56[c] | only one isomer | | |
| $Au(H_2O)_2^+$ | 0.4 ± 0.1<br>0.68[c] | 1.95 ± 0.15<br>2.09[b]<br>1.98[c] | | 0.10 |
| $Au(H_2O)_3^+$ | | 1.0 ± 0.2<br>0.73[b] | 0.28 ± 0.06<br>0.40[b] | 0.58 |
| $Au(H_2O)_4^+$ | | 0.9 ± 0.2<br>0.88[b] | 0.27 ± 0.06 | 0.55<br>0.55 |
| $Au(H_2O)_5^+$ | | 0.8 ± 0.15 | 0.25 ± 0.05 | 0.50 |
| $Au(H_2O)_6^+$ | | 0.7 ± 0.15 | 0.20 ± 0.04 | 0.45 |
| $Au(H_2O)_7^+$ | | 0.45 ± 0.1 | 0.18 ± 0.04 | 0.45 |
| $Au(H_2O)_8^+$ | | 0.45 ± 0.1 | 0.18 ± 0.04 | 0.45 |
| $Au(H_2O)_9^+$ | | 0.45 ± 0.1 | 0.18 ± 0.04 | 0.45 |
| $Au(H_2O)_{10}^+$ | | 0.45 ± 0.1 | 0.18 ± 0.04 | 0.45 |

[a] These quantities, together with the relative abundance of the "low coordination" isomer in the beam are the best fit parameters that have allowed to calculate the cross sections shown in Figure 6. The last column, labeled % gives the relative abundance of the isomer with lowest coordination number. [b] Calculations from ref 22. [c] Calculations from ref 17.

(2) The second category corresponds to the clusters $Au(H_2O)_{3...7}^+$. The cross section is significant and increases with the number of water molecules attached to the metal ion.

(3) The total CID cross section is about the same for $Au(H_2O)_{8...10}^+$ and reachs almost 100 Å$^2$ with $Au(H_2O)_8^+$ at 2.8 eV collision energy.

Figure 4 shows partial CID cross sections, corresponding to the loss of one, two, three, and four water molecules. The loss of five water molecules has not been observed under our experimental conditions. The cross sections are plotted as a function of the collision energy. It appears that the partial CID cross sections are significant when the ion resulting from the fragmentation carries at least two water molecules. The three categories drawn above when considering the total CID cross section can be observed again, although less visible.

## 4. Data Analysis

**Energy Transfer Model for Predicting Total CID Cross Sections.** This model is described extensively in ref 17. It is based on a molecular dynamics (MD) calculation which shows that helium acts as depositing energy locally into the cluster, hence, allowing for a piecewise construction of the CID process. The model can be summarized as follow:

(1) The energy transfer is impulsive. Hence, the amount of energy transferred into the cluster is a fraction of the collision energy. Collision energy thus appears as a scaling factor.

(2) The energy transfer to the entire cluster appears as the sum of local energy transfers toward each atom (or ion) forming the cluster.

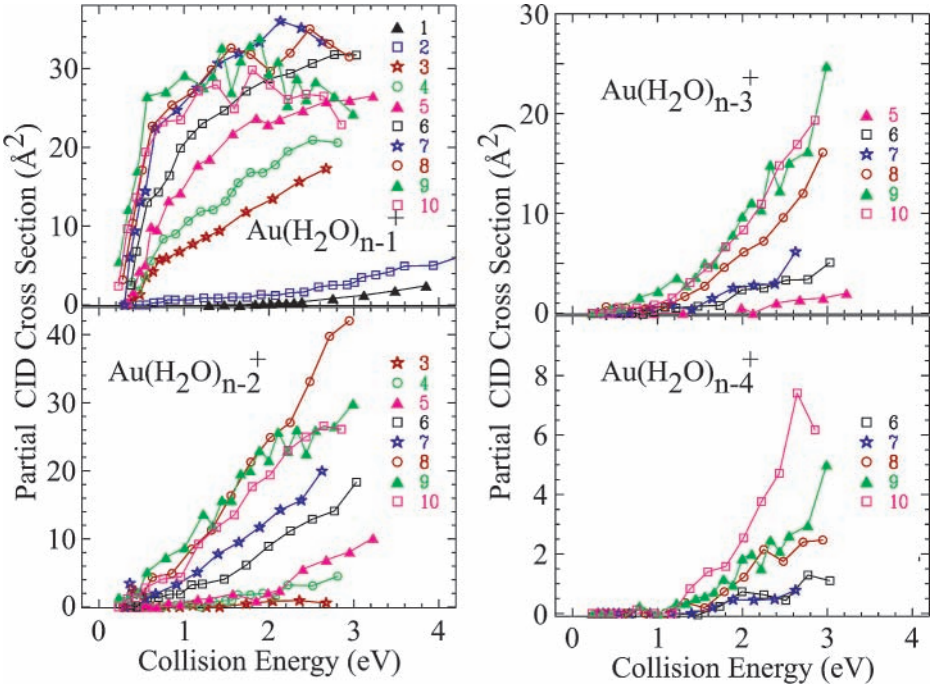


**Figure 4.** Partial CID cross section for the loss of one, two, three, and four water molecules as labeled in each panel of the figure. Otherwise, it is the same caption as Figure 3.

(3) The MD calculation has sampled trajectories where helium is collided with the cluster. The trajectories were sorted into a series of histograms that give the number of trajectories corresponding to the transfer of a specific fraction of the collision energy toward one of the atoms or ion of the cluster.

(4) Four classes of histograms were found, whether helium collides the $Au^+$ ion, an O atom, a H atom that is H-bonded to an O atom, or a H atom that is not H-bonded. The shape of the histograms differ from one class to the other. In particular, the maximum energy transfer is not the same: up to 90% of the collision energy can be transferred to a non-H-bonded H atom, whereas up to ca. 60% can be transferred to either an O atom or a H-bonded H atom. Only 1.2% can be transferred to the $Au^+$ ion.

(5) The horizontal scale of each histogram represents the fraction of energy transferred into the cluster by the collision. When multiplied by the collision energy, this scale thus corresponds to an absolute amount of energy. The vertical scale is the number of trajectory leading to the energy transfer specified by the horizontal axis. It is related directly to absolute cross sections given that each trajectory amounts for $5.2 \times 10^{-3}$ Å$^2$ in the MD calculation (sampling of one trajectory every $5.2 \times 10^{-3}$ Å$^2$ of the surface where the trajectories are started).

(6) When the amount of energy transferred into the cluster is larger than the binding energy of a water molecule, then a dissociation may occur. Under the assumption that the dissociation occurs actually, the corresponding number of trajectories gives the absolute value of the total CID cross section at this collision energy. Changing the collision energy in the calculation allows one to predict the energy dependence of the total CID cross section.

From this model, it appears that each atom forming the cluster acts as an "energy receptor" and therefore has an elementary contribution to the total CID cross section. The four classes of atoms described by the above-mentioned histograms lead to the elementary CID cross sections as suggested in the last point above. The results are shown in the top panel of Figure 5 where the elementary cross sections are plotted as a function of the collision energy. However, advantage is taken in the figure that the collision energy is a scaling factor. Hence, the energy scale is not expressed in absolute units but in reduced units were the collision energy $E_{\mathrm{Coll}}$ is divided by the binding energy of the water molecule that is to be lost:

$$E_{\mathrm{Reduced}} = \frac{E_{\mathrm{Coll}}}{\text{binding energy}} \qquad (3)$$

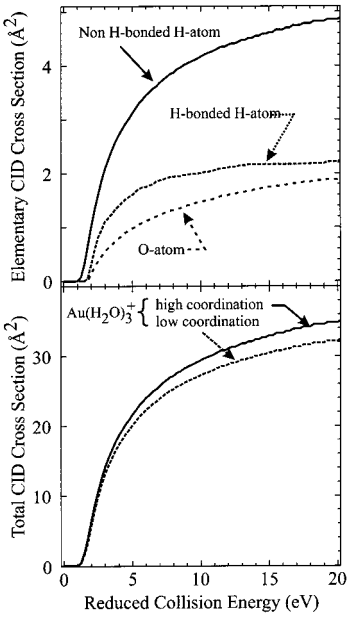


**Figure 5.** Total CID cross section calculated using the energy transfer model. The top panel shows the elementary cross sections corresponding to helium colliding H-bonded H atoms, non-H-bonded H atoms, or O atoms as labeled in the figure. The bottom panel shows the CID cross section of the $Au(H_2O)_3^+$ ion, for either its "high coordination" (three water molecules in the first solvation shell) or its "low coordination" (only two water molecules in the first solvation shell) isomer as labeled in the figure. The horizontal scale is a reduced energy scale where the collision energy is divided by the binding energy of the water molecule that is to be lost by the cluster.

As expected, the largest contribution to the CID cross section is from the H atoms that are not involved in a H bond. Up to 90% of the collision energy can be transferred indeed into these atoms, and the corresponding contribution to the total CID starts raising up near the expected threshold energy ($E_{\text{Reduced}} = 1$). Expectedly also, the contribution from the O atom and the H-bonded H atom is effective when $E_{\text{Reduced}} > 1.7$, in agreement with the about 60% energy transfer to these atoms. The energy transfer to the $Au^+$ ion is very small, because of its very large mass, and this ion does not contribute to the total CID cross section.

To get the total CID cross section, one just has to count the atoms of each class in the cluster under consideration and sum the elementary cross sections accordingly. In our previous work,[17] we used a different procedure to calculate the total CID cross section. We summed the histograms first according to the number of atoms of each class, thus providing the histogram of energy transfer to the full cluster. Then, the CID cross section was calculated. The present procedure is equivalent to this one because all of the transforms that are used to get the CID cross section are linear operations. We prefer the new procedure because the elementary cross section given in reduced energy units in the top panel of Figure 5 is more meaningful for total CID than the histograms shown in ref 17.

The four curves of Figure 5 are used now to predict the cross section of the total CID for the $Au(H_2O)_n^+$ cluster ions. A structure must be assumed in order to determine which summation of the elementary cross sections must be performed. For instance, two isomers of the $Au(H_2O)_3^+$ cluster can be considered: a "high coordination" isomer with the three water molecules directly bonded to the ion (the coordination number is 3 for the $Au^+$ ion) and a "low coordination" isomer with only two water molecules in the first solvation shell (the coordination number of $Au^+$ is 2) and the third water molecule in the second solvation shell. Besides the three O atoms and the $Au^+$ ion, the former isomer contains six non-H-bonded H atoms, whereas the second isomer contains one H-bonded H atom and five non-H-bonded H atoms. The CID cross section calculated for these isomers is plotted in the bottom panel of Figure 5. Not surprisingly, the cross section increases above the threshold more rapidly for the "high coordination" isomer than for the other. The "high coordination" isomer indeed has one non-H-bonded H atom more than the other isomer and this atom acts as a better "receptor" of the collision energy. It must be noticed that the difference between the two curves is not very large, indicating that the structural effect is not very important when the CID cross section is plotted on a reduced energy scale, suggesting that the pure structural effect is small. Of course, because both isomers are not associated with the same binding energy of water (see below), the effect of switching from one isomer to the other is dramatic when plotting the CID cross sections with the collision energy given in absolute energy units.

**Analysis of the Total CID Cross Sections.** It appears from the above paragraph that assigning a structure to the $Au(H_2O)_n^+$ cluster and a binding energy to the first water molecule that is to be lost allows one to predict both the absolute value and the energy dependence of the total CID cross section. Structures and binding energies can therefore be used as parameters to fit the experimental results of Figure 3. Except for $Au(H_2O)^+$, such fits cannot be performed so simply because the beam contains several isomers of the $Au(H_2O)_n^+$ clusters.

In practice, the fit to the experimental data has been performed, assuming two kinds of isomers for each $Au(H_2O)_n^+$ cluster with $n \geq 2$. One is called "low coordination", and the other one is called "high coordination". The two isomers of $Au(H_2O)_2^+$ correspond to both water molecules in the first solvation shell for the "high coordination" isomer (a coordination number of 2) and to one water molecule in the first shell and the second in the second shell for the "low coordination" isomer (a coordination number of 1). These isomers have already been considered in our former work where they were called "compact" and "filament", respectively.[17] The data analysis performed in this work is used again here. The incremental binding energy of water in these isomers is given in Table 1 together with the relative abundance of the "low coordination" isomer.

The situation is increasingly more complex for the larger clusters because more than two isomers may be imagined. Fortunately, the theoretical work of Feller et al.[22] on the $Au(H_2O)_{1-4}^+$ ions gives clues to simplify the situation. They have shown that the most stable isomers of the $Au(H_2O)_3^+$ and $Au(H_2O)_4^+$ ions have respectively the structures $(H_2O)Au^+(H_2O)(H_2O)$ and $(H_2O)(H_2O)Au^+(H_2O)(H_2O)$. This corresponds to the formation of two water filaments about the gold ion, which keeps a coordination number of only 2. We assume that this is still the case for larger clusters, and the isomer that we call "low coordination" has therefore the structure $(H_2O)_p(H_2O)Au^+(H_2O)(H_2O)_{n-p-2}$, with $n - 2$ H-bonded H atoms and $n + 2$ non-H-bonded H atoms. The immediately less stable isomer of $Au(H_2O)_4^+$ has three water molecules in the first solvation shell according to Feller et al.[22] This corresponds to transferring one of the terminal water molecules of the "low coordination" isomer into the first solvation shell. Then, the coordination number of gold is 3. We assume that this is still the case whatever the size of the cluster, and the "high coordination" isomer that is considered here has three water molecules in the first solvation shell. It has therefore $n - 3$ H-bonded H atoms and $n + 3$ H atoms that are not H-bonded. Following the work of Feller et al for the $Au(H_2O)_{3,4}^+$ clusters, we also assume that the binding energy of water in the "high coordination" isomer of $Au(H_2O)_{\geq 3}^+$ is smaller than in the "low coordination" isomer (0.40 versus 0.73 eV for $Au(H_2O)_3^+$).[22] With this in mind, we have fitted the experimental total CID cross sections. The best parameters, incremental binding energies, and abundance of the "low coordination" isomer are listed in Table 1. The quality of the fit is shown in Figure 6 (see the curves labeled $\sigma_{\text{tot}}$ and the open circles). Except for the $Au(H_2O)_8^+$ and $Au(H_2O)_{10}^+$ clusters, the fit goes within the experimental error bars.

**Predicting Partial CID Cross Sections.** Predicting partial CID cross sections can be done very simply, using the parameters given in Table 1, when assuming that multifragmentation is a sequential process. The energy transfer model provides us with the absolute amount of energy transferred into the cluster, as a function of the collision energy. As said above, when counting all of the trajectories leading to an energy transfer larger than the binding energy of a water molecules, then the cross section $\sigma_{\text{tot}}$ of total CID is deduced. Similarly, when the amount of energy transferred falls between the energy required for the loss of one molecule and that for the loss of two, then the partial cross section $\sigma_{-1}$ for the loss of one molecule only is deduced. Similarly the cross sections $\sigma_{-2}$, $\sigma_{-3}$, and $\sigma_{-4}$ for the loss of 2, 3, and 4 can be calculated when bracketing the amount of energy transfer by the energy needed to kick off 2, 3, 4, and more water molecules. Doing so assumes implicitly that, within the time window of the experiment, water molecules that are energetically allowed to leave the cluster sequentially actually do so, without time window effects.

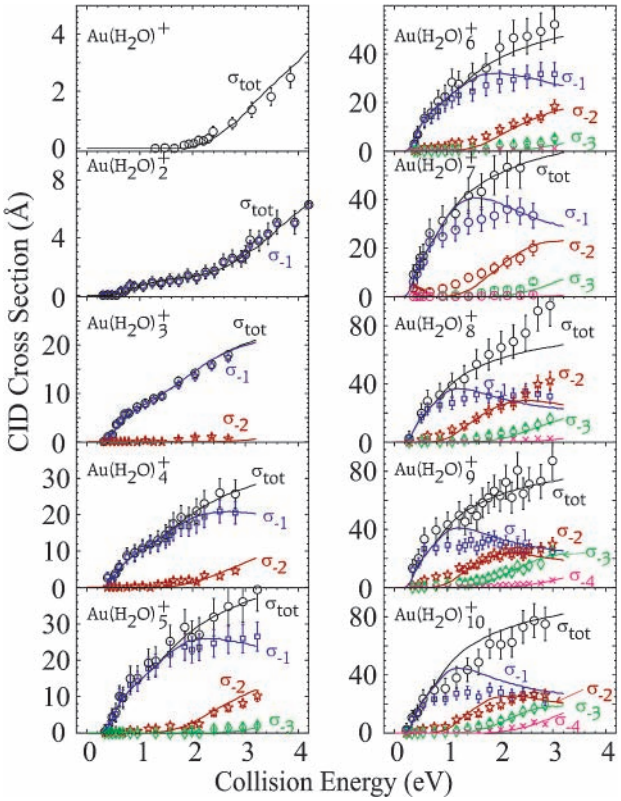


**Figure 6.** Total and partial CID cross sections for the $Au(H_2O)_n^+$ cluster ions as labeled in the figure. The symbols and error bars give the experimental data: total CID cross section $\sigma_{-tot}$ (open circles), loss of one water molecule $\sigma_{-1}$ (open squares), loss of two water molecules $\sigma_{-2}$ (open stars), loss of three water molecules $\sigma_{-3}$ (open diamonds), and loss of four water molecules $\sigma_{-4}$ (crosses). The curves are the prediction of the energy transfer model based on the molecular dynamics calculation of ref 17.

The calculation of the cross sections $\sigma_{-1}$, $\sigma_{-2}$, $\sigma_{-3}$, and $\sigma_{-4}$ has been performed, assuming that the loss of one water molecule from the $Au(H_2O)_p^+$ cluster gives the most stable $Au(H_2O)_{p-1}^+$ cluster, i.e., the "low coordination" isomer of $Au(H_2O)_{p-1}^+$ when $p \geq 4$ and the "high coordination" isomer when $p = 3$. The cross sections that have been calculated accordingly are also shown in Figure 6 and compared to the experimental results. In contrast with total cross sections, where the curves passing through the experimental points are fits, the curves corresponding to partial cross sections are predictions assuming that the multifragmentation process is sequential. Several disagreements are observed between the calculated curves and the experimental results, especially in the middle energy regime between 0.5 and 2 eV. This will be discussed later.

## 5. Discussion

We first discuss the information extracted from the fit to the total CID cross section, i.e., the binding energies listed in Table 1.

**$Au(H_2O)^+$ and $Au(H_2O)_2^+$.** The results for $Au(H_2O)^+$ and $Au(H_2O)_2^+$ have already been discussed in ref 17. Briefly, the value of 1.74 ± 0.1 eV found for the $Au(H_2O)^+$ is in excellent agreement with the binding energy $\Delta D_e$ calculated by Feller et al.[22] (1.74 eV, in an estimated complete basis set (CBS) CCSD(T) limit). It slightly overestimates the value of 1.56 eV that we have obtained in ref 17 in a calculation at the CCSD(T)/MP2 level corrected for BSSE. A good agreement is found also for the "high coordination" isomer of $Au(H_2O)_2^+$ between the measured value (1.95 ± 0.15 eV) and the calculations (1.98[17] and 2.09 eV[22]). The incremental binding energy of water in the "low coordination" structure of this cluster is much weaker: 0.4 ± 0.1 eV, slightly below our calculation in ref 17 (0.63 eV). The remark made in the Introduction about the term "H bond" must be outlined here. The value that has just been found for the "H-bonded" water molecule in the "low coordination" structure (0.4 ± 0.1 eV) is indeed almost twice the binding energy of water in the water dimer where bonding is the archetype of a H bond (0.23 ± 0.02 eV[27,28]). This is an indication that bonding between the two water molecules in the "low coordination" dimer is not purely a H bond. Polarization of the first shell water molecule by the positive gold ion and interaction of the second shell water molecule with the ion also participate to the bonding.

**$Au(H_2O)_3^+$.** The landscape changes when switching from $Au(H_2O)_2^+$ to $Au(H_2O)_3^+$. The calculations of Feller et al showed indeed that the "high coordination" structure with three water molecules in the first solvation shell is not the most stable isomer of $Au(H_2O)_3^+$ and does not have the largest incremental binding energy for water.[22] Instead, the most stable isomer of this cluster is found to be formed of a $(H_2O)Au^+(H_2O)$ core solvated by additional water molecules H-bonded to one of the core water molecules. This situation is certainly a consequence of the rather high ionization energy of gold (9.22 eV[25]) which allows for a substantial charge transfer toward the water molecules (comparatively, the ionization energy of water is 12.6 eV[25]). Similar situations where "low coordination" structures are favored have been encountered in other systems, for instance $I(H_2O)_n^+$ which develops the $(H_2O)I^+(H_2O)$ core.[26] Again, this corresponds to a situation where the solvated species (I) has a large ionization energy (10.45 eV).[25]

The incremental binding energy of water, $\Delta D_e$, calculated by Feller et al for "high coordination" $Au(H_2O)_3^+$ is 0.40 eV (6-31+G*/ECP+f basis at the RHF level), whereas it is 0.73 eV for the "low coordination" isomer (an estimated CBS calculation at the CCSD(T) level).[22] These values are in fair agreement with the corresponding values listed in Table 1 respectively 0.28 ± 0.06 and 1.0 ± 0.2 eV. Several reasons can be anticipated to account for this ordering in the isomer binding energies.

(1) The addition of a second shell water molecule stabilizes more efficiently the charge-transfer configuration $(H_2O)Au-(H_2O)^+$ than $(H_2O)Au^+(H_2O)$. As a result, adding a water molecule in the second shell favors the structure $(H_2O)Au-(H_2O)^+(H_2O)$.

(2) The "high coordination" structure with three first shell water molecules is destabilized by the unfavorable arrangement of the dipole moments of the three water molecules, which are enhanced with respect to that of free water by polarization because of the central ion core.

(3) Finally, partial hybridization of the $5d^{10}$ electron configuration of $Au^+$ as $5d^9$ 6s in the interaction with the two first shell water molecules is another cause for destabilizing the "high coordination" structure.

These three reasons may explain (i) why the incremental binding energy of water in the "low coordination" isomer is almost four times the binding energy of water in the water dimer where the bonding is the archetype of a "true H bond" (0.23 ± 0.02 eV[27,28]) and (ii) why the binding energy of water in the "high coordination" isomer is only marginally larger than the H-bond strength in the water dimer (0.28 ± 0.06 versus 0.23 eV).

**$Au(H_2O)_4^+$.** The situation that is encountered with $Au(H_2O)_4^+$ is comparable to that just discussed with $Au(H_2O)_3^+$. The "low coordination" structure leads to a water binding energy, $0.9 \pm 0.2$ eV. It is much larger than the energy of a "true H bond" and is in very nice agreement with the calculations by Feller et al (0.98 eV in an estimated CBS calculation at the CCSD(T) level). From this calculation, the stable configuration of the $Au(H_2O)_4^+$ ion involves two water chains and corresponds to the structure $(H_2O)(H_2O)Au^+(H_2O)(H_2O)$, i.e., a structure with one water molecule on each side of the $(H_2O)Au^+(H_2O)$ core. The outer water molecules that can be lost from this structure have an equivalent position to that of the water molecule which is lost by the "low coordination" $Au(H_2O)_3^+$. Not surprisingly, almost the same water binding energy is found in both "low coordination" $Au(H_2O)_3^+$ ($1.0 \pm 0.2$ eV) and "low coordination" $Au(H_2O)_4^+$ ($0.9 \pm 0.2$ eV).

The incremental binding energy of water in "high coordination" $Au(H_2O)_4^+$ was not documented in the calculation by Feller et al.[22] We found a value of $0.27 \pm 0.06$ eV that is very close to that found for "high coordination" $Au(H_2O)_3^+$ ($0.28 \pm 0.06$ eV).

**"Low Coordination" Isomers of $Au(H_2O)_{\geq 5}^+$.** No theoretical information is available for the $Au(H_2O)_n^+$ when $n \geq 5$. The trend observed in Table 1 for the "low coordination" isomer is quite interesting: the water binding energy decreases regularly from $Au(H_2O)_3^+$ ($1.0 \pm 0.2$ eV) to $Au(H_2O)_6^+$ ($0.7 \pm 0.15$ eV) by equal steps of 0.1 eV. Then a larger descending step of 0.25 eV leads to the $Au(H_2O)_{7-10}^+$ clusters, which are associated with the same incremental binding energy of water ($0.45 \pm 0.1$ eV).

The steady decrease of the water binding energy might well be associated with the saturation of the four equivalent second shell solvation sites about the $(H_2O)Au^+(H_2O)$ core, with some destabilization being due to the unfavorable dipole−dipole interaction of the second shell water molecules. According to this picture, "low coordination" $Au(H_2O)_6^+$ would appear as having two strongly polarized water molecules in the first solvation shell forming the ion core to which four water molecules forming the second solvation shell are bonded by *enhanced H bonds*. This situation resembles very much to that encountered by Jiang et al. in the protonated water clusters $H(H_2O)_n^+$ cluster:[29] the most stable $H(H_2O)_6^+$ cluster ion has the structure labeled 6II in ref 29, with four water molecules H-bonded to the four outer H atoms of the symmetric $(H_2O)H^+(H_2O)$ core (the equivalent to the present $(H_2O)Au^+(H_2O)$ core).

Only up to four water molecules can be H-bonded to the "low coordination" core $(H_2O)Au^+(H_2O)$. Hence, additional water molecules should start filling a third solvation shell. A smaller binding energy is expected, thus accounting for the 0.25 eV drop in the water binding energy when switching from $Au(H_2O)_6^+$ to $Au(H_2O)_7^+$. Considering that the binding energy of water in this third solvation is still twice the binding energy of the water dimer ($0.45 \pm 0.1$ versus $0.23 \pm 0.02$ eV[27,28]), we infer that there is a fair amount of charge transfer from the first solvation shell to the second.

No evolution of the water binding energy is observed from $Au(H_2O)_7^+$ to $Au(H_2O)_{10}^+$ ($0.45 \pm 0.1$ eV), an indication that the third solvation offers a number of equivalent sites. It is quite hard to anticipate structures for this shell without the help of high quality ab initio data. Nevertheless, several points can be brought. In particular, we do not imagine that the third solvation shell can be built simply from a H-bond network where the O atoms act as single H-atom acceptors. More complex ring structures where a water molecule of the third shell is bridging two water molecules of the second shell can be imagined. In such bridging water molecules, the O atom acts as a double H-atom acceptor, a situation which seems to be quite common and which has been documented in a number of systems, for instance in alkali$(H_2O)_{n\geq 3}^+$,[30] $NH_4(H_2O)_{5,6}^+$, [31−35] and $H(H_2O)_{5\leq n\leq 8}^+$ cluster ions.[29]

The calculation of ref 29 on the $H(H_2O)_{\geq 6}^+$ cluster ions can serve as a guide line for the present discussion. We have recalled already that $H(H_2O)_6^+$ is formed from a solvation shell of four water molecules about the $(H_2O)H^+(H_2O)$ core [which can be thought as equivalent of the present "low coordination" core $(H_2O)Au^+(H_2O)$]. Interestingly, when one more water molecule is added, the most stable configurations of $H(H_2O)_7^+$ has a five-membered water ring with a bridging water molecule (structure 7VI in ref 29). The incremental binding energy for this cluster is 0.43 eV, i.e., very close to the binding energy that is found in the present work for $Au(H_2O)_7^+$ ($0.45 \pm 0.1$ eV, see Table 1). Interestingly, also the incremental binding energy is 0.43 eV for $H(H_2O)_8^+$, but in that case, the eighth water molecules does not build a second five-membered ring at the opposite side of the cluster (structure 8III in ref 29. Instead, the eighth water molecule acts as a single H acceptor and is bonded to one of the H atoms of the bridging water molecule.

**"High Coordination" Isomers of $Au(H_2O)_{\geq 5}^+$.** The incremental binding energies read in Table 1 for the "high coordination" isomer of $Au(H_2O)_{\geq 5}^+$ are very small, in the range of 0.2 eV. A possible reason for that has been given already for $Au(H_2O)_3^+$: destabilization because of unfavorable disposition of the water dipole moments.

An additional reason may be invoked to explain why the binding energies listed in Table 1 for $Au(H_2O)_{7-10}^+$ are smaller than the binding energy in the water dimer ($0.18 \pm 0.04$ eV for $Au(H_2O)_{7-10}^+$ versus $0.23 \pm 0.02$ eV for the water dimer[27,28]). This might be an effect of the internal temperature of the cluster. Indeed, a cluster temperature of 100 K and only 10 active degrees of freedom ($Au(H_2O)_{10}^+$ has in fact 87 degrees of freedom, only the weakest of which can be populated at 100 K) can account for almost 0.1 eV of internal energy in the cluster which biases the CID threshold by the same amount. The binding energy in the "high coordination" isomers of the $Au(H_2O)_{7-10}^+$ clusters might then be close to the binding energy of the water dimer.

**Discussion of the Partial CID Cross Sections.** The discussion is turned now to the comparison between experimental and predicted partial CID cross section. Only the fragmentation channel corresponding to the loss of one water molecule is visible for $Au(H_2O)_{\leq 3}^+$, and no partial CID cross sections need to be discussed in this case. A significant loss of two and more water molecules, which deserve the discussion of partial cross sections, is observed for $Au(H_2O)_{\geq 4}^+$.

A nice agreement is observed between the measured partial cross sections and the predicted one for $Au(H_2O)_4^+$ and $Au(H_2O)_5^+$. The agreement is good also, within the limits of the error bars, for $Au(H_2O)_6^+$.

For $Au(H_2O)_7^+$ and larger clusters, a significant disagreement is observed between the calculations and the experimental results. In particular, the calculation overestimates the partial cross section $\sigma_{-1}$ at collision energies ranging between 0.7 and 1.8 eV. As a compensation because the total CID cross section is well reproduced by the calculation over this energy range, the partial cross section $\sigma_{-2}$ is underestimated by the calculation. We recall that the calculation of $\sigma_{-2}$ assumes that the loss of two water molecules is sequential, and interestingly, the energy

range of disagreement, 0.7−1.8 eV, is overlapping the threshold energy region of the $\sigma_{-2}$ curve. In particular, a measurable cross section $\sigma_{-2}$ is observed below the energy threshold for the sequential loss. This is especially visible for $Au(H_2O)_7^+$ and $Au(H_2O)_9^+$. This likely indicates that of the two water molecules are lost partly as a water dimer, thus reducing the energy threshold by 0.23 eV (0.23 eV is the binding energy between the two water molecules in the dimer).

Similarly, the cross section $\sigma_{-3}$ is slightly underestimated by the calculation for $Au(H_2O)_{8-10}^+$ in the energy range overlapping the threshold energy for the sequential loss of three water molecules. As above, this suggests that the loss can occur as the loss of a water dimer + water molecule or as a water trimer.

Facing a situation where the sequential loss of several water molecules compete with the loss of a water dimer (or trimer), an interesting issue would be to determine which kind of isomer ("low" or "high" coordination) stimulates one process over the other. The answer cannot be given from the experimental results directly, but could be the motivation for dynamics calculations that would be very challenging in view of the long time-scale (in terms of MD calculations) that is required to actually observe the multifragmentation process.

## 6. Conclusion

A beam of mass selected $Au(H_2O)_n^+$ ($n = 1-10$) cluster ions has been generated using a source that couples laser evaporation, supersonic expansion, and tandem time-of-flight mass spectrometry. These ions have been collided and fragmented by helium in the energy range 0.2−3 eV. The clusters lose a maximum of four water molecules, whatever their size in the range that has been explored.

The key point in this work is the data analysis procedure where the total and partial CID cross section have been simulated using a model of the energy transfer between helium and the cluster. This model which was introduced in a former work of this laboratory tells that the energy transfer is local and allows for a piecewise construction of the CID cross section. Each piece corresponds to the contribution of one of the atoms forming the cluster for transferring a fraction of the collision energy into the cluster. This construction of the cross section turns out to be a valuable tool for predicting the absolute value and the energy dependence of both total and partial CID cross sections when the structure and the binding energies have been assumed for the $Au(H_2O)_n^+$ cluster. This provides a tool for fitting the experimental data and give insight into the structure and energetic of the $Au(H_2O)_n^+$ clusters.

Two kinds of isomers were found for the clusters carrying two and more water molecules. One kind is a "low coordination" corresponding to the $Au^+(H_2O)(H_2O)$ structure for $Au(H_2O)_2^+$ and tentatively assigned to $(H_2O)_pAu^+(H_2O)_{n-p}$ structures for the $Au(H_2O)_{n\geq 3}^+$ clusters. The other kind is more highly coordinated. It is deduced from the "low coordination" by transferring one of the terminal water molecule as a first shell water molecule, thus giving a structure with three water molecules directly bonded to the gold ion. Interestingly, the binding energy of the water molecule that is to be lost from the "high coordination" isomer is close to the binding energy of the water dimer. In contrast, even for the largest cluster explored here, $Au(H_2O)_{10}^+$, the binding energy of water in the "low coordination" isomer is twice (or more for the smaller clusters) the binding energy of the water dimer.

Examination of the multifragmentation reveals a competition between the sequential loss of several water molecules and the loss of small water clusters. Sequential loss is the rule for the $Au(H_2O)_{3-5}^+$ clusters where the measured partial cross sections are well reproduced by the energy transfer model. Besides this mechanism, larger clusters that lose two and more waters are dimers (and may be trimers). In that case, the energy transfer model overestimates the partial cross section for the loss of one water molecule and underestimate that for the loss of two and more. This effect is especially visible in the 0.5−1.5 eV range, close and slightly above the threshold for the sequential loss of two and three water molecules.

**Acknowledgment.** The authors acknowledge the C.E.A. that has supported this work under the Grant "Interaction ion métallique molécule". They also wish to thank Philippe Millié for fruitful discussions on the nature of the bond between metal ions and water.

## References and Notes

(1) Fuke, K.; Hashimoto, K.; Iwata, S. *Adv. Chem. Phys.* **1999**, *110*, 431.
(2) Schulz, C. P.; Haugstatter, R.; Tittes, H. U.; Hertel, I. V. *Phys. Rev. Lett.* **1986**, *57*, 1703.
(3) Higashide, H.; Kaya, T.; Kobayashi, M.; Shinohara, H.; Sato, H. *Chem. Phys. Lett.* **1990**, *171*, 297.
(4) Willey, K. F.; Cheng, P. Y.; Bishop, M. B.; Duncan, M. A. *J. Am. Chem. Soc.* **1991**, *113*, 4722.
(5) Fuke, K.; Misaizu, M.; Sanekata, K.; Tsukamoto, K.; Iwata, S. *Z. Phys. D* **1993**, *26*, 180.
(6) Chang, X. Y.; Ehlich, R.; Hudson, A. J.; Polanyi, J. C.; Wang, J. X. *J. Chem. Phys.* **1997**, *106*, 3988.
(7) Lu, W.; Yang, S. *Int. J. Mass Spectrom. Ion Process* **1998**, *000*, 000.
(8) Elhanine, M.; Dukan, L.; Maître, P.; Breckenridge, W. H.; Massick, S.; Soep, B. *J. Chem. Phys.* **2000**, *112*, 10912.
(9) Donnelly, S. G.; Farrar, J. M. *J. Chem. Phys.* **1993**, *98*, 5450.
(10) Beyer, M.; Berg, C.; Görlitzer, H. W.; Schindler, T.; Achatz, U.; Albert, G.; Nieder-Schatteburg, G.; Bondybey, V. E. *J. Am. Chem. Soc.* **1996**, *118*, 7386.
(11) Dukan, L.; del Fabbro, L.; Pradel, P.; Sublemontier, O.; Mestdagh, J. M.; Visticot, J. P. *Eur. Phys. J. D* **1998**, *3*, 257.
(12) Shukla, A. K.; Futrell, J. H. *J. Mass Spectrom.* **2000**, *35*, 1069.
(13) Rodgers, M. T.; Armentrout, P. B. *Mass Spectrom.* **2000**, *19*, 215.
(14) Rodgers, M. T.; Ervin, K. M.; Armentrout, P. B. *J. Chem. Phys.* **1997**, *106*, 4499.
(15) Rodgers, M. T.; Armentrout, P. B. *J. Chem. Phys.* **1998**, *109*, 1878.
(16) Poisson, L.; Pradel, P.; Lepetit, F.; Réau, F.; Mestdagh, J. M.; Visticot, J. P. *Eur. Phys. J. D* **2001**, *14*, 89.
(17) Poisson, L.; de Pujo, V.; Brenner, A.-L.; Derepas, J. M.; Dognon, J.-P.; Mestdagh, J. M., submitted to *J. Phys. Chem. A* **2001**.
(18) Poisson, L.; Dukan, L.; Sublemontier, O.; Lepetit, F.; Reau, F.; Pradel, P.; Mestdagh, J. P.; Visticot, J. P. *Int. J. Mass Spectrom.* **2001**, Submitted.
(19) Hrušák, J.; Schroder, D.; Schwarz, H. *Chem. Phys. Lett.* **1994**, *225*, 416.
(20) Schröeder, D.; Hrušák, J.; Hertwig, R. H.; Koch, W.; Schwerdtfeger, P.; Schwarz, H. *Organometallics* **1995**, *14*, 312.
(21) Schroder, D.; Hrusak, R. H.; Pyykkö, P. *Inorg. Chem.* **1998**, *37*, 624.
(22) Feller, D.; Glendening, E. D.; de Jong, W. A. *J. Chem. Phys.* **1999**, *110*, 1475.
(23) Brechignac, C.; Cahuzac, P.; Concina, B.; Leygnier, J.; Villard, B. *AIP Conference Proc.* **2001**, *561*, 184.
(24) Sublemontier, O.; Poisson, L.; Pradel, P.; Mestdagh, J. M.; Visticot, J. P. *J. Am. Soc. Mass Spectrom.* **2000**, *11*, 160.
(25) Weast, R. C.; Astle, M. J.; Beyer, W. H. *Handbook of Chemistry and Physics*, 65th ed.; CRC Press: Boca Raton, FL, 1984.
(26) Achatz, U.; Fox, B. S.; Beyer, M. K.; Bondybey, V. E. *J. Am. Chem. Soc.* **2001**, *123*, 6151.
(27) Curtiss, L. A.; Frurip, D. J.; Blander, M. *J. Chem. Phys.* **1979**, *71*, 2703.
(28) Reimers, J. R.; Watts, R. O.; Klein, M. L. *Chem. Phys.* **1982**, *64*, 95.
(29) Jiang, J.-C.; Wang, Y.-S.; Chang, H.-C.; Lin, S. H.; Lee, Y. T.; Niedner-Schatteburg, G.; Chang, H.-C. *J. Am. Chem. Soc.* **2000**, *122*, 1398.
(30) Glendening, E. D.; Feller, D. *J. Phys. Chem.* **1995**, *99*, 3060.
(31) Wang, Y. S.; Chang, H. C.; Jiang, J. C.; Lin, S. H.; Lee, Y. T. *J. Am. Chem. Soc.* **1998**, *120*, 8777.
(32) Chang, H. C.; Wang, Y. S.; Lee, Y. T. *Int. J. Mass Spectrom.* **1998**, *180*, 91.
(33) Jiang, J. C.; Chang, H. C.; Lee, Y. T.; Lin, S. H. *J. Phys. Chem. A* **1999**, *103*, 3123.